

PAPER

Role of metallic-like conductivity in unusual temperature-dependent transport in n-ZnO : Al/p-Si heterojunction diode

To cite this article: Mohit Kumar *et al* 2015 *J. Phys. D: Appl. Phys.* **48** 455301

View the [article online](#) for updates and enhancements.

You may also like

- [Efficient light incoupling into silicon thin-film solar cells by anti-reflecting MgO/high-compact-AZO with air-side textured glass](#)
Dong-Won Kang, Heon-Min Lee and Min-Koo Han
- [Investigation of material properties and thermal stabilities of magnetron-sputter-deposited ZnO:Al/Ag/ZnO:Al transparent conductive coatings for thin-film solar cell applications](#)
Stella Van Eek, Xia Yan, Weimin Li et al.
- [The Ag layer thickness effect on the figure of merit of the AZO/Ag bilayer prepared by DC sputtering of AZO and thermal evaporation method of Ag](#)
Azarmidokht Bahadoran and Nasser Zare-Dehnavi



The Electrochemical Society
Advancing solid state & electrochemical science & technology

243rd ECS Meeting with SOFC-XVIII

Boston, MA • May 28 – June 2, 2023

**Abstract Submission Extended
Deadline: December 16**

[Learn more and submit!](#)

Role of metallic-like conductivity in unusual temperature-dependent transport in n-ZnO:Al/p-Si heterojunction diode

Mohit Kumar¹, S K Hazra² and Tapobrata Som¹

¹ SUNAG laboratory, Institute of Physics, Sachivalaya Marg, Bhubaneswar 751 005, India

² Department of Physics and Materials Science, Jaypee University of Information Technology, Waknaghat 173234, Himachal Pradesh, India

E-mail: tsom@iopb.res.in

Received 10 June 2015, revised 20 August 2015

Accepted for publication 28 August 2015

Published 6 October 2015



Abstract

The current–voltage characteristics of an n-ZnO:Al(AZO)/p-Si heterojunction diode is investigated over a temperature range of 293 and 423 K. The measured current–voltage characteristics show good rectification behaviour at all temperatures. It is observed that the AZO/Si heterojunction exhibits different (unusual) types of charge conduction processes in the temperature range under consideration. In addition, temperature-dependent resistivity measurements performed on a AZO thin film grown on a glass substrate show metallic-like conductivity, which is explained on the basis of local annealing of defects, mainly vacancies, in the AZO layer. Finally, based on our experimental findings, we construct a parametric phase diagram to elucidate the transition from one to the other conduction mechanism. The present study will be useful to understand the effect of self-heating for AZO-based devices.

Keywords: thin films, oxide heterostructures electrical transport, vacancy formation

(Some figures may appear in colour only in the online journal)

1. Introduction

ZnO is a good candidate for fabricating solar cells, heterojunction diodes, and photodetectors due to its wide band gap, ($E_g \sim 3.4$ eV at room temperature), large binding energy (60 meV), and high transparency [1]. Generally, ZnO exhibits *n*-type conductivity which can be enhanced up to three to four orders of magnitude after doping with group-III elements, especially Al-doping [2–4]. This enhanced conductivity makes ZnO:Al (AZO) a suitable material not only for transparent conducting electrodes but also for various other applications, namely ultra-violet detectors, junction diodes, etc [4–10]. Generally, AZO-based device fabrication is studied in the simplest form of an *n*-AZO/p-Si heterojunction diode [4] where the performance of the heterojunction mainly depends on factors like the growth process, Al-doping, and the working temperature of the devices [2]. Recently, it has been reported that the charge transport property of ZnO and doped-ZnO materials changes significantly with temperature.

For instance, temperature-dependent metallic-like behaviour has been reported for ZnO, AZO, and Ga-doped ZnO thin films deposited on insulating substrates [11, 12]. This unusual change in resistivity with temperature is expected to play an important role in the charge transport process of a device based on doped-ZnO systems. However, the role of temperature-dependent resistivity of AZO in the current–voltage (*I*–*V*) characteristics of an AZO-based heterojunction diode is still lacking. Thus, in order to use AZO/Si heterojunctions for device applications, a detailed understanding of changes occurring in its *I*–*V* characteristics due to external heating is exigent.

In this regard, it may be mentioned that often AZO-based heterojunctions are operated at high current densities (beyond the turn-on potential, V_T), which causes self-heating to occur in the device. This is expected to bring variation in the junction characteristics which can affect the device performance to a significant extent. It is envisaged that changes occurring in the *I*–*V* characteristics of the heterojunction due to self-heating

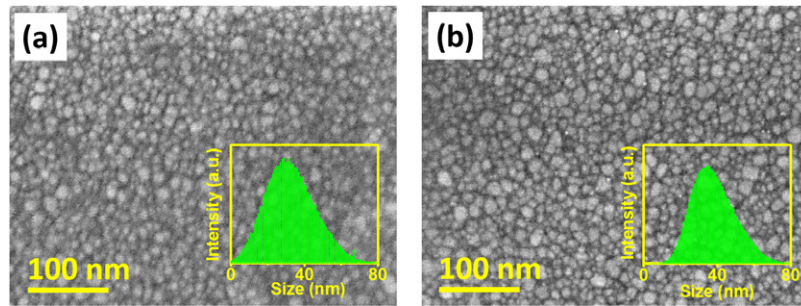


Figure 1. (a), (b) Plan-view SEM images before and after heat treatment, respectively. The insets show the grain size distributions of the corresponding film.

should be similar to those observed under the influence of external heating. Therefore, it is important to investigate temperature-dependent changes in the resistivity of AZO thin films and its effect on the performance of n-AZO/p-Si heterojunction diodes.

In this paper, we investigate the effect of temperature on the transport mechanism of an n-AZO/p-Si heterojunction diode. A large variation in the I - V characteristics with temperature is observed. In particular, temperature-dependent transition from direct tunnelling to thermionic emission is observed in the I - V characteristics. In order to explain this behaviour, temperature-dependent resistivity of AZO film, deposited on soda-lime glass (SLG) substrate, is also investigated. The measured resistivity reveals a semiconducting nature at low temperatures (up to 343 K), which subsequently transforms into a metallic-like behaviour at higher temperatures (>343 K). In addition, we have made use of optical absorption spectroscopy before and after temperature treatment, which shows a reduction in the band gap of the AZO layer. These observations are discussed in terms of annihilation of oxygen vacancies in the AZO layer.

2. Experimental

AZO films of an optimized thickness of ~ 60 nm were simultaneously deposited on ultrasonically cleaned SLG and native oxide covered p-type Si(100) substrates at room temperature (RT) using a pulsed dc magnetron sputtering system. Commercially available 99.99% pure ZnO:Al₂O₃ (2 wt%) target (50.8 mm diameter \times 6.35 mm thick) was used to deposit AZO thin films. Ultra-pure (99.999%) argon gas was injected into the chamber with a flow rate of 27 sccm to maintain the working pressure of 5×10^{-3} mbar during sputtering. A pulsed dc power of 100 W (frequency = 150 kHz, reverse time = 0.4 μ s) was applied to the AZO target, and the substrates (kept at a fixed target-to-substrate distance of 8 cm) were rotated with a speed of 3 rpm to achieve uniform film thickness.

Microstructural changes in the AZO films before and after heat treatment were monitored by scanning electron microscopy (SEM) (Carl Zeiss) in the plan-view geometry and using 5 keV electrons. The crystallinity and phase identification of AZO films were performed by x-ray diffraction (XRD) (Bruker, D8-Discover) studies using the Bragg-Brentano

geometry and the Cu-K α radiation ($\lambda = 0.1542$ nm). Silver paste (SPI) was used to make electrical contacts on top of the AZO film and back side of the Si substrate. An indigenously developed sample holder assembly (having a heating stage), whose temperature was precisely controlled (± 0.5 K) by a proportional-integral-derivative temperature controller and sensed by a platinum resistance temperature detector (RDT, A class) thermocouple, was coupled with a source meter (Keithley 2410) to perform the temperature-dependent electrical studies. The I - V data were recorded using commercially available software (Lab-Tracer 2.0) during annealing (293–423 K) of the AZO/Si heterojunctions in air. In addition, the optical absorption of AZO films before and after temperature treatment was measured by a UV-visible-NIR spectrophotometer (Shimadzu, 3101PC) in the wavelength range of 300–700 nm. The reproducibility of the results were confirmed on three different AZO thicknesses, namely 40, 60, and 120 nm.

3. Results and discussion

AZO films were analysed by SEM and XRD to look for a possible correlation between the charge transport and structural properties of the films. Figures 1(a) and (b) show SEM images of an AZO film deposited on Si substrate before and after the heat treatment. It is observed that in both cases AZO film shows a granular nature, albeit the average grain size increases from 30 nm to 35 nm and the width of grain size distribution decreases (respective inset of figures 1(a) and (b)). In fact, as the temperature increases, thermal energy increases the diffusion of atoms and in turn smaller grains merge into a bigger grain.

Figure 2 shows the XRD pattern of an AZO film grown on Si which confirms the crystalline nature of the film. The dominant peak at $2\theta = 34.1^\circ$ can be attributed to the (002) reflection of the hexagonal wurtzite structure, indicating the formation of highly oriented grains along the c -axis [2, 3, 13]. The average grain size is determined using Scherer's formula: $D = 0.9\lambda/\beta \cos \theta$ where D is the crystallite size, β is the full width at half maximum, θ is Bragg's angle, and λ is the Cu-K α x-ray wavelength [2, 3, 13]. Thus, the average grain size of the film before and after heat treatment is found to be 17 nm and 21 nm, respectively. Further, a small shift (0.08°) in the peak position is observed. It is known that an XRD peak shift towards a lower 2θ value with respect to the bulk ZnO can be attributed

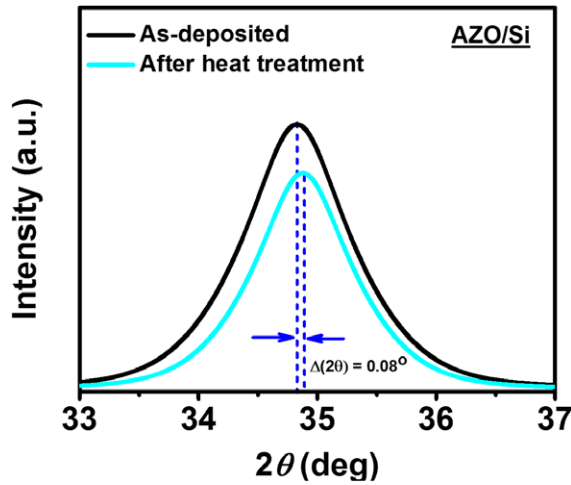


Figure 2. XRD patterns of an AZO film before and after heat treatment.

to the existence of compressive stress in the film, originating from oxygen implantation during the sputtering process [3]. In-plane film stress is calculated on the basis of the biaxial strain model: $\sigma = [2C_{13} - C_{33}(C_{11} + C_{12})/C_{13}] \times (c - c_0)/c_0$ where elastic stiffness constants are: $C_{11} = 2.1 \times 10^{11} \text{ N m}^{-2}$, $C_{33} = 2.1 \times 10^{11} \text{ N m}^{-2}$, $C_{12} = 1.2 \times 10^{11} \text{ N m}^{-2}$, and $C_{13} = 1.05 \times 10^{11} \text{ N m}^{-2}$ [2, 3]. Using the above values, σ turns out to be $-4.5 \times 10^{11}(c - c_0)/c_0 \text{ N m}^{-2}$. For a hexagonal lattice with (002) orientation, $c = 2d_s$ and $c_0 = 2d_0 = 0.5206 \text{ nm}$ where d_s is the inter-planar spacing derived from the (002) peak position and d_0 is the corresponding one for the stress-free system (0.2603 nm). In addition, one can derive the film strain using the relation: $[(d_s - d_0)/d_0] \times 100\%$. The measured strain and stress values for the as-deposited AZO film are found to be $-4.27 \times 10^9 \text{ N m}^{-2}$ and -0.98% , respectively, which are in good agreement with our previous report [3]. However, this decreases to $-4.20 \times 10^9 \text{ N m}^{-2}$ and -0.92% , respectively, indicating a relaxation of stress in the film due to heat treatment. Further, it may be mentioned that similar SEM and XRD behaviours are observed for the film deposited on glass substrates (data not shown).

Figure 3(a) shows the I - V characteristics of an n-AZO/p-Si heterojunction diode at different temperatures, varying from 293 to 423 K, where all I - V curves show the rectifying property. It is evident from this figure that both forward and reverse currents are not only dependent on the applied voltage but also on the sample temperature. Theoretically, the V_T of a semiconductor heterojunction diode should decrease with increasing temperature [14]. However, the present I - V data show unusual variation, where no significant change takes place in V_T with increasing temperature in the range of 293–343 K, while it increases beyond 343 K (table 1). The similar trend is observed in the reverse saturation current (I_s) as well (table 1). The value of the ideality factor (n), determined from the slope of the linear region of the forward bias $\log(I$ - $V)$ characteristics [15], has a typical value of 2.1 ± 0.1 . The values of n and series resistance (R_s) at all temperatures are calculated from the corresponding I - V characteristics and are summarized in table 1.

To understand the mechanism behind the variation in I - V characteristics more clearly, we have plotted the data using

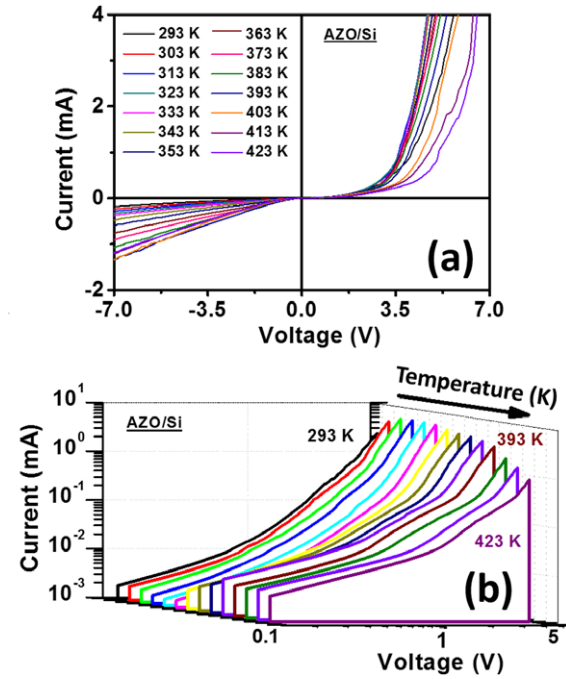


Figure 3. (a) Temperature-dependent I - V characteristics of AZO/Si heterojunction diode, (b) log-log plots of the forward bias characteristics of (a) where the arrow indicates the direction of increasing temperature.

a log-log scale [15, 16]. The log-log I - V characteristics of a heterojunction under forward bias from 293 to 423 K are shown in figure 3(b). In this figure, two interesting features are worth noting: (i) the current values at low voltages ($<0.5 \text{ V}$) show inconsistency with increasing temperature; and (ii) a clear hump at higher temperatures is observed for intermediate voltages ($0.6 < V < 1.2$). In fact, the behaviour up to a certain applied voltage ($\sim 0.6 \text{ V}$) is Ohmic and thereafter non-Ohmic behaviour is manifested due to thermal effects which indicates defect activation and an increase in the electrical current [17]. For a better clarity, the log-log plot of I - V data, measured at 373 K, is shown in figure 4. As a result, a change in the behaviour of the I - V characteristics at different voltages becomes very clear. In fact, the I - V plot can be divided into four different regimes as described below. Region-I: current is linearly dependent on voltage, i.e. Ohmic in nature, region-II: exponentially dependent on voltage, region-III: shows a power law dependence, $I \propto V^a$ where $a > 1$, and region-IV: there is a sudden enhancement in current with voltage [18–20]. These four regions in the I - V characteristics are also strongly influenced by temperature, which is a signature of the thermally activated charge injection mechanism [18–20]. However, at lower temperatures ($<343 \text{ K}$), the I - V curves show a weak temperature-dependence, which can be well described by the tunnelling mechanism [18–20]. Generally, temperature-dependent I - V characteristics are explained in the framework of Schottky-type conduction and/or space charge limited conduction [18]. However, the anomaly in our results indicates that possibly different conduction mechanisms are operative in different voltage-temperature regimes.

Figure 5(a) shows $\ln(I)$ versus $V^{1/2}$ behaviour to establish the main current conduction mechanism in the n-AZO/p-Si

Table 1. Diode parameters extracted from temperature-dependent I - V data.

S.N.	Sample temperature (K)	Turn on potential, V_T (V)	Reverse leakage current, I_0 (mA)	Series resistance (Ω)	Ideality factor, n
1	293	3.48	0.32	444.62	2.04
2	303	3.45	0.28	342.19	2.05
3	313	3.45	0.24	317.05	2.06
4	323	3.44	0.19	313.53	2.05
5	333	3.43	0.32	303.24	2.03
6	343	3.50	0.40	309.99	2.03
7	353	3.54	0.50	333.91	2.10
8	363	3.62	0.78	367.11	2.12
9	373	3.71	0.92	444.76	2.15
10	383	3.91	1.02	514.88	2.19
11	393	4.25	1.13	466.79	2.15
12	403	4.56	1.16	372.35	2.14
13	413	5.12	1.01	349.41	2.13
14	423	5.43	1.10	350.46	2.11

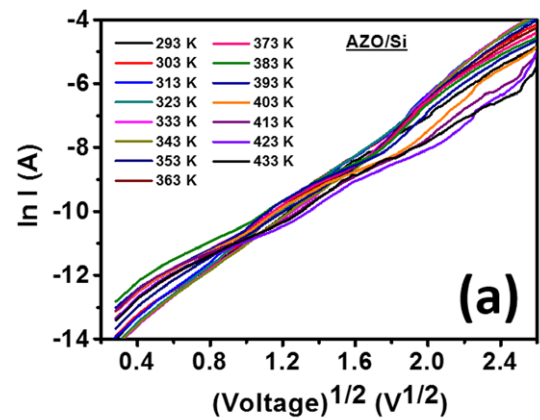
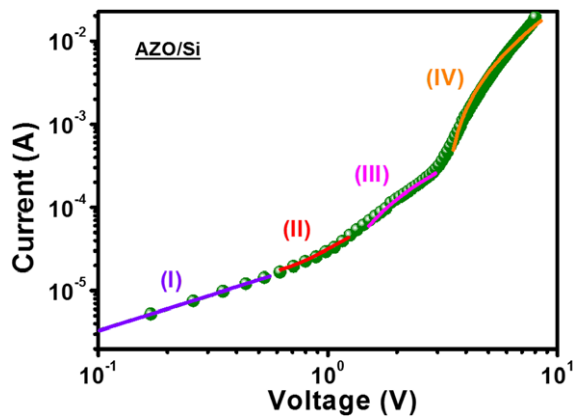


Figure 4. Log-log I - V plot under the forward bias corresponding to 373 K where (I), (II), (III), and (IV) show different conduction regimes.

heterojunction diode and these curves are further used to calculate the reverse saturation current. It is observed that $\ln(I)$ versus $V^{1/2}$ curves remain linear at lower voltages (<0.6 V) but deviate at higher voltages (>0.6 V), ruling out the possibility of a Schottky-type conduction mechanism at higher voltages [21, 22]. In addition, by extrapolating straight lines (not shown in the figure) to 0 V (figure 5(a)), we obtain the leakage current (I_0) as a function of temperature, which is further used to calculate the barrier height (Φ) at the AZO/Si interface. For the calculation of Φ , $\ln(I_0/T^2)$ is plotted as a function of $1000/T$ in figure 5(b), which reveals a linear relation at higher temperatures (>383 K). However, the plot remains constant below 383 K, indicating a weak temperature-dependence at lower temperatures. In fact, the constant value of $\ln(I_0/T^2)$, up to 383 K, indicates that current at low bias voltages (<0.6 V) is governed by direct tunnelling [21]. For this voltage regime, the current is described by the relation:

$$I \propto V \exp\left[-2d\sqrt{2m^* \Phi_B}/\hbar\right], \quad (1)$$

where \hbar is reduced Planck's constant, m^* is effective mass of the charge carrier, d is the width of the interface barrier, and Φ_B is the junction barrier height [22, 23]. However, at higher

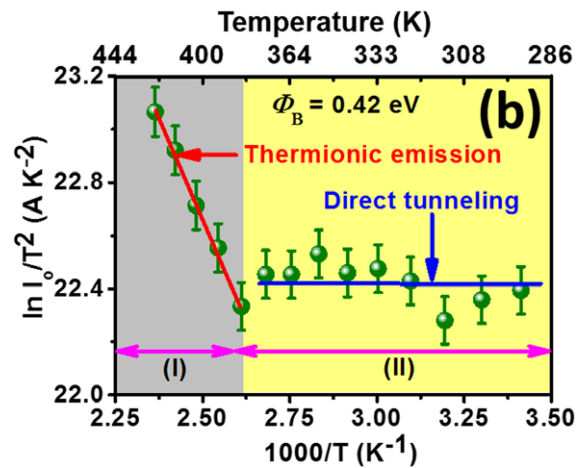


Figure 5. (a) $\ln(I)$ versus $V^{1/2}$ plot, (b) Arrhenius plot extracted from (a) for the AZO film deposited on the Si substrate.

temperatures, thermionic emission governs the charge transport process. The I - V characteristics in this regime obey the Richardson-Schottky equation and the current is described by the relation:

$$I = A * T^2 \exp\left[-\left\{\Phi_B - \sqrt{\left(\frac{q^3 V}{4\pi\epsilon_0\epsilon_r d}\right)}\right\}/k_B T\right], \quad (2)$$

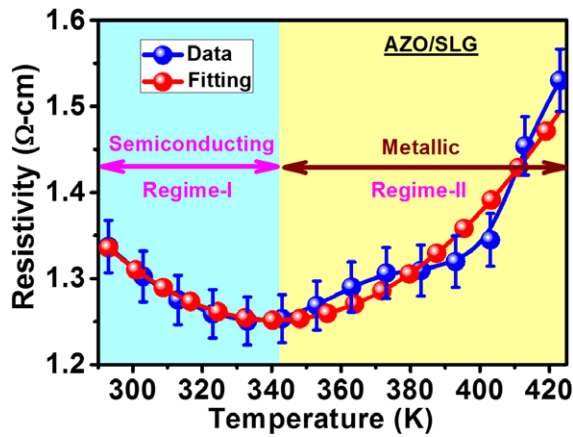


Figure 6. Temperature-dependent resistivity of an AZO film deposited on the SLG substrate.

where A^* is the effective Richardson constant, ϵ_r is the permittivity of AZO film, ϵ_0 is the permittivity of vacuum, and q is the electronic charge [18]. The thermionic regime also shows a variation in the leakage current, I_0 . A subsequent calculation of the junction barrier height corresponding to the thermionic regime reveals an activated behaviour due to the high value of $\Phi_B = 0.42$ eV. In fact, when the temperature is low (383 K), thermal energy of the charge carriers is low, which is not sufficient to overcome this barrier height. This indicates that different mechanisms are operative at different temperatures [22].

Recently, it has been reported that electrical properties of ZnO and doped-ZnO change with an increase in temperature, which play a significant role in electrical transport [11, 12]. To understand the unusual I - V behaviour of the AZO/Si heterojunction described above, we have carried out resistivity measurements of an AZO thin film at different temperatures. Figure 6 shows the temperature-dependent resistivity of the AZO film deposited on a glass substrate. Interestingly, the experimental resistivity values show two different regimes: initially the resistivity decreases with temperature (<343 K) and thereafter, it increases at higher temperatures (≥ 343 K). The initial decreasing trend in regime-I (highlighted by the cyan-coloured block) can be correlated to the semiconducting nature of the AZO film, whereas the subsequent trend in regime-II (highlighted by the yellow-coloured block) is in contradiction since it resembles the metallic behaviour. It is observed from this figure that the resistivity of the AZO film at 423 K is higher in comparison to that at RT (293 K). In addition, the resistivity of AZO film is also measured after bringing down the furnace temperature to RT which is found to be the same as 423 K, indicating the irreversible nature of the metallic-like behaviour. Interestingly, it is observed that the AZO film after heat treatment has bigger grain sizes and less compressive strain and hence should have low resistivity. However, the resistivity increases after heat treatment which indicates that some other mechanism is responsible for this behaviour.

Normally, Al acts as an effective donor either by substitution at the Zn sites or by creating oxygen vacancies after sitting as an interstitial atom, which in turn leads to the low

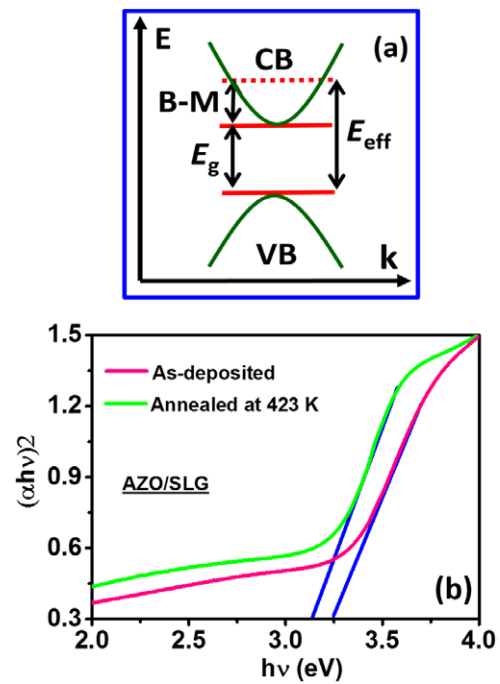


Figure 7. (a) Schematic representation of Burstein–Moss (B–M) shift, (b) the measured band gap of an AZO film (deposited on the SLG substrate) before and after heat treatment.

resistivity of AZO films [2, 24]. In addition, these donor electrons (due to Al or oxygen vacancies), normally occupy the higher (deeper) energy levels in the conduction band, which in turn can initiate high energy photon absorption during the optical studies. As a result, the effective band gap (E_g) of an AZO film should be relatively higher when compared to the separation between the minima (of the conduction band) and the maxima (of the valence band) of this direct band gap semiconductor (shown in figure 7(a)). Such a widening in the band gap is known as a Burstein–Moss shift which depends on the carrier density of the film, n , according to $n^{2/3}$ [25]. It is well-known that electrical transport properties of AZO can be understood on the basis of optical absorption study. Thus, to understand the observed metallic-like behaviour of the AZO film, we have performed the optical absorption before and after the heat-treatment. Since the heat treatment is performed in air, oxygen adsorption in AZO film is likely to happen. This can lead to a more stoichiometric nature of the AZO film due to the annihilation of oxygen vacancies, causing a decrease in the carrier concentration [11]. As a consequence, the band gap of the AZO film after heat treatment should be lower relative to the as-deposited one. Thus, to understand the reason behind the metallic-like conductivity, we have measured the energy gaps of the AZO film from the optical absorption spectra. It is observed that after annealing at 443 K, the absorption edge shifts towards a lower energy (3.27 to 3.13 eV) (figure 7(b)). This behaviour can be attributed to the fact that at relatively lower temperatures (<383 K), oxygen atoms do not get absorbed at the surface because of insufficient activation energy, whereas beyond 383 K, the atmospheric oxygen atoms interact with the surface and in turn reduce the carrier density in the films. In fact, due to annealing in open air, electrons

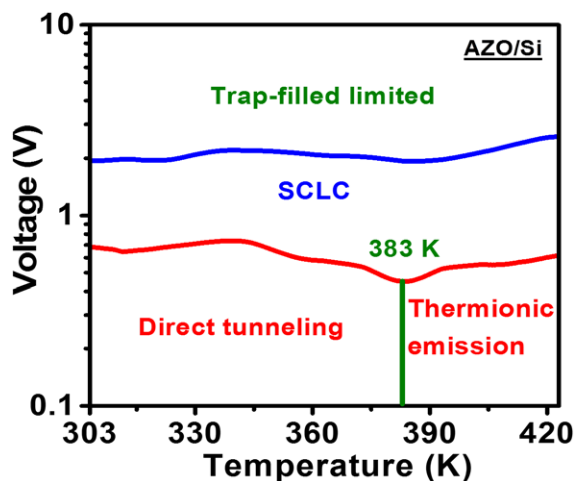


Figure 8. Voltage versus temperature parametric phase diagram for a n-AZO/p-Si heterojunction diode.

get accumulated at the AZO surface and can be trapped by oxygen molecules to form negatively charged oxygen ions [26]. These trapped electrons lead to a reduction in the effective donor density within the oxide.

A similar behaviour has been reported in the case of Ga-doped ZnO after annealing which confirms the reduction in oxygen vacancies [12]. To fortify this fact, similar heat treatment on AZO film, deposited on glass substrate, is performed in vacuum (8×10^{-8} mbar) and subsequent change in the band gap (absorption spectra not shown) is measured. Interestingly, no change in the optical band gap is observed which confirms that annihilation of oxygen vacancies is responsible for the metallic-like behaviour of the AZO film under consideration. Therefore, the variation in resistivity of the AZO film has a one-to-one correspondence with the I - V characteristics of n-AZO/p-Si heterojunction. Based on the above discussion, we can infer that the temperature-dependent charge conduction mechanism in the AZO/Si heterojunction diode is primarily governed by the AZO layer.

Based on our experimental observations, we have constructed a parametric phase diagram (voltage versus temperature) which defines the dominating charge conduction mechanism at a fixed temperature (figure 8). It is clear from this diagram that at lower temperatures the conduction mechanism is governed by diffusion; however, this changes to the thermionic emission process beyond a certain temperature. The reproducibility of these results were checked on five different AZO samples (60 nm thick) grown on both Si and SLG substrates. Interestingly, similar behaviour is observed for three different AZO film thicknesses, namely 40, 60, and 120 nm, grown on both SLG and p-Si substrate. Thus, we conclude that the present study will provide important input to understand the effect of self-heating of AZO-based devices operating at high temperatures.

4. Conclusions

In summary, we have deposited AZO films on SLG and p-Si substrates and performed temperature-dependent I - V studies.

I - V characteristics of n-AZO/p-Si heterojunction diodes at different temperatures reveal unusual behaviour, which is correlated with the temperature-dependent resistivity of the AZO film deposited on the SLG substrates. At higher temperatures, an increase in the resistivity takes place which is attributed to the annihilation oxygen vacancies. The metallic-like conductivity of the AZO film, at relatively higher temperatures, is concluded to be responsible for the transition of the conduction mechanism from diffusion to the thermionic emission mode. The present study will enable us to address the self-heating effect on AZO-based devices.

Acknowledgment

The authors would like to thank Dr Pratap Sahoo (NISER, Bhubaneswar) for extending SEM setup.

References

- [1] Ellmer K 2008 *Transparent Conductive Zinc Oxide* (Berlin: Springer)
- [2] Lu J G, Ye Z Z, Zeng Y J, Zhu L P, Wang L, Yuan J and Zhao B H 2006 *J. Appl. Phys.* **100** 073714
- [3] Kumar M, Kanjilal A and Som T 2013 *AIP Adv.* **3** 092126
- [4] Basu T, Kumar M and Som T 2014 *Mater. Lett.* **135** 188
- [5] Basu T, Kumar M, Sahoo P K, Kanjilal A and Som T 2014 *Nanoscale Res. Lett.* **9** 1
- [6] Pradhan A K, Mundle R M, Santiago K, Skuza J R, Xiao B, Song K D, Bahoura M, Cheaito R and Hopkins P E 2014 *Sci. Rep.* **4** 6415
- [7] Islama M M, Ishizuka S, Yamada A, Matsubara K, Niki S, Sakurai T and Akimoto K 2011 *Appl. Surf. Sci.* **257** 4026
- [8] Kaurn G, Mitra A and Yadav K L 2015 *Prog. Nat. Sci.: Mater. Int.* **25** 12
- [9] Naik G V, Liu J, Kildishev A V, Shalaeva V M and Boltassev A 2012 *Proc. Natl Acad Sci.* **109** 8834
- [10] Sarkar S, Patra S, Bera S K, Paul G K and Ghosh R 2012 *Physica E* **46** 1
- [11] Bamiduro O, Mustafa H, Mundle R, Konda R B and Pradhan A K 2007 *Appl. Phys. Lett.* **90** 252108
- [12] Bhosle V, Tiwari A and Narayan J 2006 *Appl. Phys. Lett.* **88** 032106
- [13] He B B 2009 *Two-Dimensional X-Ray Diffraction* (Hoboken, NJ: Wiley)
- [14] Majumdar S and Banerji P 2009 *J. Appl. Phys.* **105** 043704
- [15] Kargar A et al 2013 *Nano Lett.* **13** 3017
- [16] Yang F, Wei M and Deng H 2013 *J. Appl. Phys.* **114** 134502
- [17] Asghar M, Mahmood K, Faisal M and Hasan M A 2013 *J. Phys.: Conf. Ser.* **439** 012030
- [18] Cao C W et al 2013 *ECS Solid State Lett.* **2** 25
- [19] He B, Wang H Z, Li Y G, Ma Z Q, Xu J, Zhang Q H, Wang C R, Xing H Z, Zhao L and Rui Y C 2013 *J. Alloys Compd.* **581** 28
- [20] Zhang X G and Pantelides S T 2012 *Phys. Rev. Lett.* **108** 266602
- [21] Songand D and Guo B 2009 *J. Phys. D: Appl. Phys.* **42** 025103
- [22] Sarker B K and Khondaker S I 2012 *ACS Nano* **6** 4993
- [23] Kumar M, Basu T and Som T 2015 *J. Appl. Phys.* **118** 055102
- [24] Ali G M and Chakrabarti P 2010 *Appl. Phys. Lett.* **97** 031116
- [25] Lua J G et al 2007 *J. Appl. Phys.* **101** 083705
- [26] Hoffmann M W G, Gad A E, Prades J D, Francisco H-R, Fizec R, Shen H and Mathur S 2013 *Nano Energy* **2** 514